Pre- and post-saccadic stimulus timing in Saccadic Suppression of Displacement – a computational model

Arnold Ziesche[a], Julia Bergelt[a], Heiner Deubel[b], Fred H Hamker[a,*]

[a] *Technische Universität Chemnitz, Straße der Nationen 62, 09107 Chemnitz, Germany*
[b] *Ludwig-Maximilians-Universität, Leopoldstraße 13 , 80802 München, Germany*

Abstract

When the target of a saccadic eye movement is displaced while the eyes move this displacement is often not noticed (saccadic suppression of displacement, SSD). We present a neurobiologically motivated, computational model of SSD and compare its simulation results to experimental data. The model offers a simple explanation of the effects of pre- and post-saccadic stimulus blanking on SSD in terms of peri-saccadic network dynamics. Under normal peri-saccadic conditions pre-and post-saccadic stimulus traces are recurrently integrated with reference to present and future eye position, whereas blanking diminishes the pre-saccadic stimulus trace and thus leads to an uninfluenced integration of the post-saccadic stimulus trace. We show that part of the intersubject variability in SSD can be explained by differences in decision thresholds of this integration process.

Keywords:
saccadic suppression of displacement, computational model, proprioception, corollary discharge, reference frames, coordinate transformation

1. Introduction

With each shift of our gaze, the image on the retina abruptly changes. However, we do not perceive these jumps during eye movements. Rather, the

*Corresponding author
Email address: fred.hamker@informatik.tu-chemnitz.de (Fred H Hamker)
URL: https://www.tu-chemnitz.de/informatik/KI/index.php.en (Fred H Hamker)

world appears stable to us. This phenomenon has been termed 'visual stability across eye movements'. While multiple experiments explored different aspects of visual stability, we here focus on the experimental paradigm known as saccadic suppression of displacement (SSD, e.g., Bridgeman, Hendry and Stark, 1975). It revealed that subjects are unable to perceive small perisaccadic displacements of stimuli which they can well detect when they occur during fixation. In other words, subjects perceive the world as visually more stable than it actually is.

Meanwhile, several studies addressed different aspects of SSD. Deubel, Bridgeman and Schneider (1996) found that the detectability of stimulus displacements can be considerably improved when the stimulus at the saccade target is not displaced during the saccade but first removed and then shown after a blanking period of about 250ms at its displaced position, known as the blanking or (post-)gap effect. Less attention has been given to the observation by Deubel et al. (1996) that an improvement of the detection performance also occurs when the target stimulus is not blanked after but before the saccade (pre-gap effect).

Zimmermann, Morrone and Burr (2013) found that a prolonged viewing time prior to saccade onset also improves the detection of stimulus displacements. Zimmermann et al. (2013) and Zimmermann, Born, Fink and Cavanagh (2014) further revealed that a displacement detection reduction does not require a saccade: similar decrements in performance occur during fixation if, instead of the execution of a saccade, a mask is presented.

An early theory proposed to explain the SSD effect – the object reference or visual search theory (Deubel et al., 1996; Bridgeman, 2007) states that the visual system uses visual objects, usually the stimulus at the saccade target, to recalibrate spatial perception after the saccade. According to this theory, small displacements of the saccade target are not noticed because the visual system assumes that the saccade target stays stable during the saccade and ascribes any deviances of the target which should be in the center of the fovea after the saccade to an imprecise eye movement. Only if the target displacements are too large the visual system uses other information such as proprioception to recalibrate spatial perception, which leads to the detection of the stimulus displacements. In this framework the blanking effect is explained by a spatiotemporal 'constancy' window: Only if the saccade target stimulus is found within this spatiotemporal window the world is perceived as stable. If the object reappears after this window has closed, the stability assumption is dropped and target displacements are detected (Bridgeman,

2007).

Based on a similar assumption but spelled out in a computational framework, Niemeier, Crawford and Tweed (2003) proposed a Bayesian transsaccadic integration model. They attempted to predict the perceived displacement of a stimulus by combining the stimulus position, an internal estimate of the eye positions (e.g. efference copy) and an expectation about the probability of peri-saccadic target displacements (the prior). The model rests on the assumption that the brain computes this prior for each experimental condition, while the underlying mechanisms however, are not part of the model. They fitted the model to their own recorded data by using a sharply tuned prior in the non-blanking condition and a broadly tuned one in the blanking condition.

Atsma, Maij, Koppen, Irwin and Medendorp (2016) criticised this model as it necessarily relies on the integration of a displacement vector (the combined visual and motor signals) and a prior around zero displacement. Thus, independent of the size of the true displacement it always predicts a reduction of the perceived displacement. They proposed a different model which in parallel applies not only an integration but also a separation of the pre- and post-saccadic stimuli and weighting both using the factors displacement size and viewing time to compute the final percept. They found that the degree of integration and separation depends on displacement size, where small displacements show a stronger weight for integration. However, Atsma et al. (2016) do not address the blanking condition with their model. Further, viewing time is not explicitly modeled but only implicitly in the probability density function coding the precision of the stimulus.

Understanding SSD by computing a unitary percept from pre-and post-saccadic stimulus contributions as suggested by Atsma et al. (2016) is not novel and has been already proposed in a neuro-computational model of SSD (Ziesche and Hamker, 2014), which has the further advantage that time is explicitly part of the model description. This model explains the blanking effect as an uninfluenced integration of the post-saccadic stimulus as the neural trace of the pre-saccadic stimulus has declined during the blanking period. Further, the eye dependent parameters have been fully updated at the time of post-saccadic stimulus presentation. In the non-blanking condition, both the pre- and post-saccadic stimulus, are integrated into a single percept. However, as the model has to link the pre-saccadic with the post-saccadic view it uses an egocentric reference frame based on internal eye position signals. In the non-blanking condition, the eye position signals have not

been fully updated as the displacement occurs during saccade. Ziesche and Hamker (2014) further explained how predictive remapping, first reported by Duhamel, Colby and Goldberg (1992), and corollary discharge are linked to saccadic suppression of displacement. However, the model does not require a saccade to show a reduction of displacement detection. Bergelt and Hamker (2016) applied the model to a masking experiment without a saccade and could well account for the observation of Zimmermann et al. (2014).

To further investigate the properties of the neuro-computational model, in particular with respect to variations of the stimulus timings, we applied it to the most relevant experimental variations of Deubel et al. (1996).

2. Material and methods

The neuro-computational model has been originally introduced to explain the peri-saccadic mislocalization of briefly flashed stimuli in complete darkness (Ziesche and Hamker, 2011). It has then been slightly adapted to the paradigm of saccadic suppression of displacement (Ziesche and Hamker, 2014; Bergelt and Hamker, 2016). As the model has been described in detail before, we will here describe its properties on a coarse level.

2.1. Anatomy

Our proposed model rests on the assumption that parietal areas, such as the lateral intraparietal area (LIP), receive two different kinds of eye position information (Fig. 1). First, a proprioceptive information about eye position (Andersen et al., 1990; Bremmer et al., 1997), presumably from the somatosensory cortex (Wang et al., 2007; Xu et al., 2011, 2012), and second, a preparatory corollary discharge about the intended saccade displacement (Colby et al., 1996; Wurtz, 2008; Melcher and Colby, 2008) which presumably originates in the superior colliculus (SC) and is routed via the mediodorsal nucleus (MD) and the frontal eye field (FEF, Sommer and Wurtz, 2004, 2008). However, the exact origins of these eye position signals are not critical assumptions but rather provide a source of inspiration for the model design. Importantly, both eye position signals are used to transform a visual stimulus position signal, which is encoded in a retinocentric reference frame coming from early extrastriate areas, into an intermediate reference frame. The representation of stimulus position in the intermediate reference frames is then used to compute the stimulus position in a head-centered reference frame (Galletti et al., 1995; Mullette-Gillman et al., 2005). The computation

of an explicit head-centered reference frame is not a critical requirement of the model but slightly improves the simulation results (Ziesche and Hamker, 2011, 2014).

2.2. Model

We use the concept of basis function networks (Pouget et al., 2002) to combine a retinotopic retinal signal (modeled in a one-dimensional neuron layer Xr) with proprioceptive (modelled in a 1D layer $\mathrm{Xe_{PC}}$) and corollary discharge (modeled in a 1D layer $\mathrm{Xe_{CD}}$) signals. The basis functions are realized in two two-dimensional layers $\mathrm{Xb_{PC}}$ and $\mathrm{Xb_{CD}}$ in which the retinal signal is modulated by proprioception and corollary discharge respectively. From these basis function representations we read out a head-centered stimulus representation in an output layer Xh (Fig. 2). Since we use a fully dynamic neural network based on rate-coded neurons (Hamker, 2005; Zirnsak et al., 2011) we model the time courses of the input signals realistically to obtain explanations of phenomena of peri-saccadic spatial perception which occur on fine time scales (see below). For details on the implementation of the network layers and connection patterns we refer the reader to our previous publications (Ziesche and Hamker, 2011, 2014; Bergelt and Hamker, 2016). For a simplified version of the equations describing the interactions of the model layers, see the grey boxes in Figure 2.

The continuous firing rates of the neurons at the output layer Xh are fed into a decision process based on competing, accumulating decision neurons (Usher and McClelland, 2001; Hamker, 2007) to reach a decision about the stimulus displacement (justified by Kiani et al., 2008; Stanford et al., 2010). Since we aim at replicating the findings from Deubel et al. (1996) we use a decision process with two decision neurons, one voting for a forward target displacement, the other voting for a backward target displacement. The procedure is similar to our previous application of the model (Ziesche and Hamker, 2011), however there we used a decision process which came up with spatial location percept. The details of the modified two-choice decision process are presented below.

The principle functionality of the model on the SSD task has been described previously (Ziesche and Hamker, 2014; Bergelt and Hamker, 2016), which we briefly summarize here. Our model postulates that the pre-saccadic stimulus trace is integrated with the post-saccadic stimulus trace to compute the location of a stimulus. As our model also contains feedback connections (Figure 2) any present evidence affects the processing of new evidence. Thus,

the pre-saccadic stimulus trace affects the post-saccadic processing and stabilises the percept in favour of the pre-saccadic evidence. This explains that small displacements during saccade become unnoticed. Thus, in its core SSD has similarities to visual masking. In order to align pre- and post-saccadic views egocentric reference frames in form of the two eye position signals are used. One eye position signal, the proprioceptive signal, computes the stimulus in reference of the pre-saccadic position and the other, the corollary discharge, in reference of the future eye position. The interaction of the stimulus encoded in the pre-saccadic reference frame with the corollary discharge leads to predictive remapping, i.e. the response of a neuron to a stimulus presented in its future receptive field (Ziesche and Hamker, 2014). When we selectively disrupted either predictive remapping or corollary discharge the model predicts a bias in reporting displacements opposite to the saccade direction, as the predictive component is in part or fully suppressed.

2.2.1. Timing of the physiological signals

In our previous presentation of the model (Ziesche and Hamker, 2011) where it had been applied to explain the mislocalization of brief flashes around saccades in total darkness, we presented various parameter variations of the timing of the physiological signals. Here, we choose specific values for these timings to achieve a good data fit. However, we were careful to choose parameter values which are in the range of suitable values derived from the parameter variations in (Ziesche and Hamker, 2011). Specifically, the parameters we use here produce comparable outcomes as in the previous study. We used the following timing parameters for the physiological eye position signals:

The proprioceptive (PC) eye position signal encodes the eye position during fixation but does not move with the eye during the saccade. Rather, it represents the pre-saccadic eye position during the saccade until it starts updating to the new eye position some time after saccade offset as suggested by experimental data (Wang et al., 2007; Xu et al., 2011, 2012). In our simulations, the neural activity representing the post-saccadic eye position is turned on $t_{\mathrm{PC,\,on}} = 32$ms relative to *saccade offset*. At the same time ($t_{\mathrm{PC,\,off}} = 32$ms), the activity representing the pre-saccadic eye position starts to decay. In the present study, we use a faster decay factor $\sigma_{\mathrm{PC,\,off}} = 15$ (as compared to $\sigma_{\mathrm{PC,\,off}} = 35$ in (Ziesche and Hamker, 2011)). As the eye-position is mathematically computed by a differential equation, the change needs some time to become effective, which takes additional 30-40 ms to

become fully established. Thus, the model is well consistent with the observation that proprioceptive eye position lags behind the true eye position (Wang et al., 2007; Xu et al., 2011), but the model LIP gain fields update 50-100ms earlier than those recently reported for monkeys (Xu et al., 2012). As macaque monkeys did not show any difference between blank and step trials, different than in humans (Joiner et al., 2013), a full replication of monkey data may not be a requirement to explain data of SSD experiments run with humans and we kept the parameters of the original model (Ziesche and Hamker, 2011).

The corollary discharge (CD) signal is a transient representation of the planned saccade displacement in retinotopic coordinates whose temporal dynamics are well motivated from single cell recordings in the superior colliculus, the frontal eye field and the mediodorsal nucleus (MD) of the thalamus (Sommer and Wurtz, 2004, 2008). In the present study, we use a faster decay factor $\beta_{\mathrm{CD}} = 65$ (as compared to $\beta_{\mathrm{CD}} = 150$ in (Ziesche and Hamker, 2011)). A faster decay factor in the CD signal leads to a more pronounced mislocalization opposite to the saccade direction when stimuli are flashed in total darkeness after saccade onset, which has been obseved in experimental data as well (Ziesche and Hamker, 2011). Thus, the present choice of parameters is still consistent with observations in previous studies. Further, it is also likely that decay and rise times of the CD and PC signals vary in individual subjects.

2.2.2. Details of the decision process

The computation of the input to the decision process consists of several steps (see Figure 3):

1. The input I^{DP} to the decision process consists of the firing rates of Xh, i.e. $I_i^{\mathrm{DP}} = r_i^{\mathrm{Xh}}$ when they are above a threshold of 0.04. The start time of the accumulation process is set to 28ms after saccade offset for conditions where the displaced stimulus reappears during the saccade and 60ms after stimulus onset when the displaced stimulus reappears after saccade offset. We chose not to couple the accumulation onset to stimulus onset for peri-saccadic stimuli since peri-saccadic detectability of stimuli is suppressed (Volkmann et al., 1978). The timing of 28ms after saccade offset is set to a similar timing as the updating of the proprioceptive eye position signal (see above), assuming that this signal might be used to trigger the accumulation process. The interval

between stimulus onset and accumulation onset for stimuli appearing after saccade offset is roughly set to the time where the stimulus activity reaches Xh.

2. The position information encoded in the input I^{DP} is decoded using template matching with precalculated templates of much higher spatial resolution than the number of entries in I^{DP}. Each entry codes 4 degrees. Hence the templates represent stimulus position with a step size of 0.5 degrees. Template matching is done using correlation. The match m_c of the template t_i^c representing a stimulus at position c with neurons i is

$$m_c = \sum_j r_j^{\mathrm{Xh}} t_j^c. \tag{1}$$

   The spatial resolution of the decision neurons equals the one of the templates.

3. We introduce noise by first transforming the rate coded input to a spiking neuron model using a Poisson spike train and then transforming it back to rate coded input by averaging. To be more specific, one time step of the input m_c (the template match from the previous step) is equivalent to n time steps of the spiking neuron $\tilde{m}_c$ ($n = 20$ is the bin size). Spiking is simulated in the simplest way: In each of the n time steps the neuron spikes if and only if $m_c > Rs_{\max}$ where R is a random number between 0 and 1. The spiking activity of the neuron is $s_{\max} = 1$ while the non-spiking activity is 0. Thus the activity at the spiking time step t is

$$\tilde{m}_c^t = \begin{cases} s_{\max}, & \text{if } m_c > Rs_{\max} \\ 0, & \text{else} \end{cases} . \tag{2}$$

   Then, the activity of the spiking neuron is averaged to obtain a rate.

$$m_c = \frac{1}{n} \sum_{t=0}^{n-1} \tilde{m}_c^t \tag{3}$$

4. In the previous step we introduced rate-coded neurons encoding evidence for the presence of a stimulus at each spatial position with a resolution of 0.5 degrees. In this step, we collect all these evidences into two evidences m_f and m_b, one for forward jumps and one for

backward jumps. For this we use the pre-saccadic stimulus position c_{pre} as a decision border:

$$m_f = \sum_{c \geq c_{\text{pre}}} m_c \tag{4}$$

$$m_b = \sum_{c \leq c_{\text{pre}}} m_c \tag{5}$$

5. We implement a competition between the decision neurons by subtracting each input from the other:

$$m_f := m_f - m_b \tag{6}$$

$$m_b := m_b - m_f \tag{7}$$

6. Accumulating decision neurons are implemented as in (Hamker, 2007). The ODE of each of the two decision neurons d_f and d_b is:

$$\tau^{\text{DN}} \frac{t}{dt} d_{f/b}(t) = m_{f/b} \tag{8}$$

with time step $h^{\text{DN}} = 1$, time constant $\tau^{\text{DN}} = 50$. Each decision neuron d_c is initialized with a baseline firing rate of 0.1 before the decision process begins. A decision is made when one of the neurons reaches the threshold $d_{\text{thresh}} = 0.3$ to 0.9 (the threshold is systematically varied). If none of the neurons reaches this threshold after $t^{\text{DN}}_{\text{max}} = 70$ms, the neuron with the highest activity at that time wins (see Kiani et al., 2008).

7. This whole process is repeated $c^{\text{DN}}_{\text{trials}} = 100$ times and then averaged to compute the average number of 'forward jump' responses over all trials.

2.2.3. Simulation of experimental paradigms

We simulate the experimental paradigm from Deubel et al. (1996) for four different experiments (Fig. 4). For easy reference, we use the same numbering of experiments as in Deubel et al. (1996). In all experiments, we simulate saccadic eye movements from 0° towards a stimulus at the saccade target which is presented at 8° (saccades are simulated by the saccade generator from Van Wetter and Van Opstal (2008)). In experiments I and II the target stimulus jumps once the saccade is detected by the experimental equipment.

In experiment I, the stimulus jumps either $+1^\circ$ (i.e. in saccade direction) or -1° (opposite to saccade direction). Before it reappears at its displaced position, it is blanked for a variable time from 0ms to 270ms. In experiment II, this time is set fixed to either 0ms or 250ms and the target jump is varied between -2° and $+2^\circ$. In experiment III, the stimulus is displaced immediately when the saccade is detected by $+1^\circ$ or -1° and is blanked for 250ms *after* a variable time of 0ms to 150ms. In experiment IV, the stimulus also jumps immediately when the saccade is detected by $+1^\circ$ or -1°. However, here the jump is *preceded* by a variable blanking of the stimulus from 20ms to 200ms. In other words, the stimulus disappears before saccade onset (for most conditions).

3. Results

3.1. The SSD effect

To demonstrate that our model replicates the experimental data from Deubel et al. (1996), in particular the pre-gap and post-gap effects, we replot the experimental data along with our model simulations in Fig. 5. Figure $5A$ shows that the detection performance increases with gap duration. The main SSD effect is shown in Fig. $5B$. The psychometric curves for displacement detection without target blanking (0ms gap) are shallow which indicates that small displacements are often unnoticed. The experimental data shows a large in between-subject variability. In comparison, panel C shows the performance in the blanking (post-gap) condition (250ms gap). Here, the psychometric curves are steep which indicates good detection performance. In the 0ms gap condition small displacements are not detected well and the model replicates a response bias towards positive displacements. In the model, this effect is due to various causes which can be seen in detail in the activity traces of the input and output layers of the model in Fig. 6. Long time (for example 200ms) before saccade onset the stimulus which is presented at the saccade target evokes activity in the retinal input layer Xr at a retinotopic position representing the saccade target (indicated by the horizontal green line). At the same time, proprioceptive eye position in $\mathrm{Xe_{PC}}$ encodes the pre-saccadic eye position which is 0° (indicated by the horizontal black line). The model combines these activities into a head-centered stimulus position which correctly encodes the saccade target in the output layer Xh. Closer to saccade onset (50ms before) the corollary discharge signal in

Xe_{CD} rises which leads to a distortion in positive spatial direction of the activity in Xh. Shortly after saccade onset ($10 - 20$ms) suppression in Xb_{PC} (Ziesche and Hamker, 2011) leads to reduced activity in Xh which retains for the whole saccade time. Later (around 50ms after saccade onset) the retinal input signal in Xr starts to reflect the stimulus movement on the retina in the opposite direction of the saccade (towards the negative saccade amplitude). This leads to further distortions of the head-centered output signal in Xh. Finally, shortly before the eye reaches its post-saccadic position, the decision process starts accumulating evidence from Xh (indicated by the vertical blue lines in Fig. 6). Around the same time the proprioceptive eye position signal in Xe_{PC} starts updating to the new eye position. This leads to increased activity and further distortions in Xh and also affects the still ongoing accumulation process in the decision neurons. In the end (about 200ms after saccade onset) the peri-saccadic distortions end and a correct representation of stimulus position in Xh is restored.

In sum, distortions of the stimulus representation around the decision time are due to changes in all of the input signals, the corollary discharge, the stimulus movement on the retina, and the proprioceptive eye position signal. The feedback connections from Xh to Xb_{CD} stabilize the activity pattern in Xh such that the disturbances of the input signals do not affect the activity pattern in Xh immediately but only slowly. Thus, also peri-saccadic stimulus displacements do not influence Xh immediately but only later in the accumulation process where they have a weaker effect. Together, the peri-saccadic distortions of Xh due to updates in the input signals and the stabilization of Xh due to feedback loops explain the SSD effect.

3.2. The blanking effect

One main finding of Deubel et al. (1996) is the so called blanking effect, i.e. that detection performances for stimulus displacements are completely restored when the displacement does not occur immediately during the saccade, but after a blanking period of the stimulus. Figure 7 shows the activity traces for a blanking period of 250ms. Although the peri-saccadic distortions in Xh are the same as in the no-gap condition (Figure 6), they have ceased at the time where the activity of the post-gap stimulus enters the system (indicated by the vertical blue line). Hence, stimulus position is immediately represented correctly in Xh.

3.3. The pre-gap effect

The second main finding of Deubel et al. (1996) is the so called pre-gap effect. Here they show that the detection performance is not only restored for post-saccadic stimulus blanking but also for pre-saccadic stimulus blanking. Our model is able to replicate this effect (Figure $5E$). It offers an explanation in terms of its feedback loops. With a long pre-saccadic gap there is no previous activity in the head-centred output layer Xh when the displaced stimulus enters the system. Thus, any response of Xh to the new stimulus – although potentially distorted – immediately reflects the displaced stimulus position. In other words, when the pre-gap is a long enough, the detection performance might still be biased but displacements are detected well (i.e. the psychometric curve is steep).

3.4. The effect of the decision threshold

The behavioral data from Deubel et al. (1996) shows intersubject variability in most experiments. Remarkably, the variability in the model for different decision thresholds is very similar to the one of the subjects (Fig. 8). We will now describe how the decision threshold influences the SSD effect using the no-gap condition (Fig. $8B$). Figure 9 shows the activities of the decision neurons for three different thresholds in the 0ms gap, 0° target displacement condition. As the main effect of the decision threshold the decision times increase (indicated by the circles at the end of the lines). Furthermore, for longer decision times the accumulated evidence changes. While the evidence for a forward displacement is stronger in the first period of about 10-20ms, later (20-40ms) the evidence for a backward displacement is stronger. Thus, longer decision times are predicted to lead to tendency to decide for backward displacements.

Since the model performance varies in the same range as the subjects' performance (Fig. 8), we were interested whether it is possible to assign each subject a model threshold which explains the subjects' data well across all experiments. To this end, we compared each subject's performance with each threshold's performance separately for all experiments using the mean square error (Fig. 10). Indeed we found that subjects could be assigned with at least a range of likely thresholds. For example, subject OS shows a performance similar to the model with a threshold of 0.6-0.7. Subject AM is close to thresholds of 0.7-0.8 except for experiment II with 250ms gap. However, in that experiment all subjects' and all thresholds' performances are almost identical anyway. Subjects TM and CE are both close to smaller

thresholds and subject CK is similar to a threshold of 0.8. In sum, at least part of the variability among the subjects can be well explained by a different integration threshold.

However, a parameter that directly counteracts with the decision threshold is the speed of the accumulation process. Thus, a variation of the strength of the CD signal (cCD in eq. 14 of Ziesche & Hamker, 2011) leads to a similar effect. Lowering a threshold is similar to speeding up the accumulation process by a stronger CD signal. Thus, behavioral data can not dissociate a variation of the decision threshold from a variation of the speed of the accumulation process.

4. Discussion

Saccadic suppression of displacement (SSD) has been explained at different levels of abstraction. The object reference theory (Deubel et al., 1996; Bridgeman, 2007) assumes a built in assumption of visual stability. It proposes a post-saccadic spatiotemporal window around the saccade target in which displacements of the target are tolerated without noticing any instability. This theory explains the target blanking effect as follows: because the target could not be found after the saccade, the assumption of stability is broken, and displacements become visible. How such proposed mechanisms may be implemented in the brain has not been discussed further.

Optimal trans-saccadic integration (Niemeier et al., 2003) formalized some of the above ideas in a Bayesian framework and suggested that peri-saccadic perception represents the optimal solution to the integration of noisy visual and extraretinal signals. One drawback, however, is the need for explaining the post-saccadic blanking effect by a change in the prior probability density distribution, which is a free parameter. Atsma et al. (2016) proposed a slightly different Bayesian model which not only integrates but also separates the pre-and post-saccadic stimulus representations. This model has not been directly tested on the blanking effect, but generally tuned to combine the pre-and post-saccadic representations of stimuli. However, the model has no internal spatio-temporal representation of the stimuli as this is beyond the mathematical formalism used.

Our model is the first that explains the SSD effect on a neural basis by simple dynamic properties of the visual system: the displacement is not perceived since the network activity of the displaced stimulus interacts with the network dynamics of peri-saccadic updating which stem from the pre-saccadic

stimulus, the corollary discharge, and proprioceptive eye position information. The head-centered representation of pre-saccadic stimulus feeds back to the incoming displaced stimulus response and stabilizes the representation in the presence of small displacements. The model can also explain the target blanking effect in which displacements become apparent when the target is blanked after the saccade: In this case, no stabilization occurs because the peri-saccadic network dynamics have been ceased. In addition, the propioceptive signal and thus the gain fields have fully updated to the present fixation position. In the case of target blanking before the saccade the activity of the target stimulus only slowly decreases in the network due to feedback connections. Thus, depending on the length of the blanking, it influences the peri-saccadic network activity to a varying amount. Our model is fully self-consistent and it does not require to make particular distinctions between the blanking and non-blanking cases. Moreover, it provides a simple explanation of the pre-gap effect in terms of network perturbations which need about 100ms to decay. Its explanation of SSD is distinct from the object reference theory since it rather relies on transsaccadic integration than on an explicit object reference. In contrast to the theory of optimal trans-saccadic integration our model does not need to make any assumptions about a priori probability distributions. Rather the observed effects in SSD emerge naturally from the time courses of the involved signals, which are grounded on physiological data.

Our comparison of model simulation results to the experimental results lead to an experimentally testable prediction. As the subjects' performance co-varies with the decision thresholds, faster decisions (i.e. induced by lower thresholds) should lead to a forward bias in the psychometric curves. Other parameters in isolation do not account for such a variation. However, we cannot rule out that the combined effects of multiple parameters may lead to a similar variation. Further, instead of a lowered decision threshold a faster accumulation process may take place. Due to the simplicity of the prediction it may be tested by looking at the reactions times in speeded responses or rather by estimating the underlying decision time (Stanford et al., 2010).

In this study we aimed to particularly address SSD with respect to variations of the stimulus timings of data from Deubel et al. (1996) which has so far not been modelled in such detail. However, the model also appears consistent with other more recent observations such as that a prolonged viewing time prior to saccade onset improves displacement detection (Zimmermann et al., 2013). This can be explained by the assumption that the decision

process in the model terminates if the integration has reached the internal threshold such that the displaced object is not being integrated with the pre-saccadic view. From this perspective SSD is not particularly about saccades but about the integration of stimuli, which if it occurs across saccades, spatial updating signals induce a particular distortion in the integration process. Similarly, we applied the model to a masking experiment without a saccade and observed comparable errors to saccade trials (Bergelt and Hamker, 2016) consistent with recent data (Zimmermann et al., 2014).

Although we have focused on modelling SSD in this study, the models' broader implication on peri-saccadic dynamics should be briefly discussed. Behavioral studies that flashed stimuli briefly around saccade onset revealed two different observations. Under illuminated conditions and the presence of references a mislocalization towards the saccade target has been observed (Ross et al., 1997; Kaiser and Lappe, 2004), whereas in total darkness the mislocalization is typically in direction of the saccade vector (Honda, 1989; Van Wetter and Van Opstal, 2008). As our model of SSD accounts also well for the data in total darkness (Ziesche and Hamker, 2011), it suggests that SSD and the mislocalization in total darkness are mediated by the same underlying mechanisms. However, the mislocalization towards the saccade target appears to rely on a different mechanism (Hamker et al., 2008, 2011).

Acknowledgements

This research has been supported by the Federal Ministry of Education and Research within the grant "Visuospatial Cognition" (BMBF 01GW0653) and partly within the program "US-German collaboration on computational neuroscience" (BMBF 01GQ1409).

References

Andersen, R.A., Bracewell, R.M., Barash, S., Gnadt, J.W., Fogassi, L., 1990. Eye position effects on visual, memory, and saccade-related activity in areas LIP and 7a of macaque. The Journal of Neuroscience 10, 1176–96.

Atsma, J., Maij, F., Koppen, M., Irwin, D.E., Medendorp, W.P., 2016. Causal inference for spatial constancy across saccades. PLoS Comput Biol 12, e1004766.

Bergelt, J., Hamker, F.H., 2016. Suppression of displacement detection in the presence and absence of eye movements: a neuro-computational perspective. Biol Cybern 110, 81–89.

Bremmer, F., Distler, C., Hoffmann, K., 1997. Eye position effects in monkey cortex. ii. pursuit- and fixation-related activity in posterior parietal areas lip and 7a. J Neurophysiol 77, 962–977.

Bridgeman, B., 2007. Efference copy and its limitations. Computers in biology and medicine 37, 924–9.

Bridgeman, B., Hendry, D., Stark, L., 1975. Failure to detect displacement of the visual world during saccadic eye movements. Vision Research 15, 719–22.

Cassanello, C.R., Ferrera, V.P., 2007. Computing vector differences using a gain field-like mechanism in monkey frontal eye field. The Journal of Physiology 582, 647–64.

Colby, C.L., Duhamel, J.R., Goldberg, M.E., 1996. Visual, presaccadic, and cognitive activation of single neurons in monkey lateral intraparietal area. Journal of Neurophysiology 76, 2841–52.

Deubel, H., Bridgeman, B., Schneider, W.X., 1996. Postsaccadic target blanking prevents saccadic suppression of image displacement. Vision Research 36, 985–96.

Duhamel, J., Colby, C., Goldberg, M., 1992. The updating of the representation of visual space in parietal cortex by intended eye movements. Science 255, 90–92.

Galletti, C., Battaglini, P.P., Fattori, P., 1995. Eye position influence on the parieto-occipital area PO (V6) of the macaque monkey. The European Journal of Neuroscience 7, 2486–501.

Hamker, F.H., 2005. The reentry hypothesis: the putative interaction of the frontal eye field, ventrolateral prefrontal cortex, and areas V4, IT for attention and eye movement. Cerebral Cortex 15, 431–47.

Hamker, F.H., 2007. The mechanisms of feature inheritance as predicted by a systems-level model of visual attention and decision making. Advances in Cognitive Psychology 3, 111–123.

Hamker, F.H., Zirnsak, M., Calow, D., Lappe, M., 2008. The peri-saccadic perception of objects and space. PLoS Computational Biology 4, e31.

Hamker, F.H., Zirnsak, M., Ziesche, A., Lappe, M., 2011. Computational models of spatial updating in peri-saccadic perception. Philosophical Transactions of the Royal Society B: Biological Sciences 366, 554–571.

Honda, H., 1989. Perceptual localization of visual stimuli flashed during saccades. Percept Psychophys 45, 162–174.

Joiner, W.M., Cavanaugh, J., FitzGibbon, E.J., Wurtz, R.H., 2013. Corollary discharge contributes to perceived eye location in monkeys. Journal of neurophysiology 110, 2402–2413.

Kaiser, M., Lappe, M., 2004. Perisaccadic mislocalization orthogonal to saccade direction. Neuron 41, 293–300.

Kiani, R., Hanks, T.D., Shadlen, M.N., 2008. Bounded integration in parietal cortex underlies decisions even when viewing duration is dictated by the environment. The Journal of Neuroscience 28, 3017–29.

Melcher, D., Colby, C.L., 2008. Trans-saccadic perception. Trends Cogn Sci 12, 466–473.

Mullette-Gillman, O.A., Cohen, Y.E., Groh, J.M., 2005. Eye-centered, head-centered, and complex coding of visual and auditory targets in the intraparietal sulcus. Journal of Neurophysiology 94, 2331–2352.

Niemeier, M., Crawford, J.D., Tweed, D.B., 2003. Optimal transsaccadic integration explains distorted spatial perception. Nature 422, 76–80.

Pouget, A., Denève, S., Duhamel, J.R., 2002. A computational perspective on the neural basis of multisensory spatial representations. Nature Reviews Neuroscience 3, 741–747.

Ross, J., Morrone, M., Burr, D., 1997. Compression of visual space before saccades. Nature 386, 598–601.

Sommer, M.A., Wurtz, R.H., 2004. What the brain stem tells the frontal cortex. I. Oculomotor signals sent from superior colliculus to frontal eye field via mediodorsal thalamus. Journal of Neurophysiology 91, 1381–402.

Sommer, M.A., Wurtz, R.H., 2008. Brain circuits for the internal monitoring of movements. Annual Review of Neuroscience 31, 317–38.

Stanford, T.R., Shankar, S., Massoglia, D.P., Costello, M.G., Salinas, E., 2010. Perceptual decision making in less than 30 milliseconds. Nature Neuroscience 13, 379–85.

Usher, M., McClelland, J.L., 2001. The time course of perceptual choice: the leaky, competing accumulator model. Psychological Review 108, 550–92.

Van Wetter, S.M.C.I., Van Opstal, A.J., 2008. Experimental test of visuomotor updating models that explain perisaccadic mislocalization. Journal of Vision 8, 8.1–22.

Volkmann, F.C., Riggs, L.A., White, K.D., Moore, R.K., 1978. Contrast sensitivity during saccadic eye movements. Vision Research 18, 1193–9.

Wang, X., Zhang, M., Cohen, I.S., Goldberg, M.E., 2007. The proprioceptive representation of eye position in monkey primary somatosensory cortex. Nature Neuroscience 10, 640–6.

Wurtz, R.H., 2008. Neuronal mechanisms of visual stability. Vision Res 48, 2070–2089.

Xu, B.Y., Karachi, C., Goldberg, M.E., 2012. The postsaccadic unreliability of gain fields renders it unlikely that the motor system can use them to calculate target position in space. Neuron 76, 1201–1209.

Xu, Y., Wang, X., Peck, C., Goldberg, M.E., 2011. The time course of the tonic oculomotor proprioceptive signal in area 3a of somatosensory cortex. Journal of Neurophysiology .

Ziesche, A., Hamker, F.H., 2011. A computational model for the influence of corollary discharge and proprioception on the perisaccadic mislocalization of briefly presented stimuli in complete darkness. J Neurosci 31, 17392–17405.

Ziesche, A., Hamker, F.H., 2014. Brain circuits underlying visual stability across eye movements-converging evidence for a neuro-computational model of area lip. Front Comput Neurosci 8, 25.

Zimmermann, E., Born, S., Fink, G.R., Cavanagh, P., 2014. Masking produces compression of space and time in the absence of eye movements. J Neurophysiol 112, 3066–3076.

Zimmermann, E., Morrone, M.C., Burr, D.C., 2013. Spatial position information accumulates steadily over time. J Neurosci 33, 18396–18401.

Zirnsak, M., Beuth, F., Hamker, F.H., 2011. Split of spatial attention as predicted by a systems-level model of visual attention. European Journal of Neuroscience 33, 2035–45.

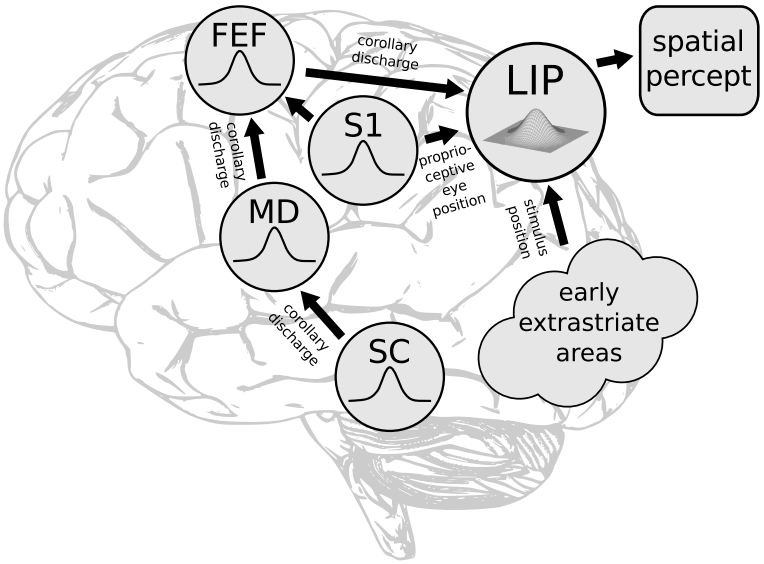

Figure 1: Putative anatomical relationship of the model to the human brain. After the initial processing of stimulus properties in early visual areas, spatial information is represented in the parietal cortex in various reference frames. The core of the model may be localized in the human homologue of the lateral intraparietal area (LIP). It receives stimulus position information in retinotopic coordinates from early extrastriate areas, proprioceptive eye position information from primary somatosensory cortex (S1), and a phasic corollary discharge signal encoding planned saccade displacement originating from the superior colliculus (SC) and routed via mediodorsal nucleus (MD) and frontal eye field (FEF) to LIP. All this spatial information is integrated in LIP and then decoded to yield a spatial percept of the stimulus position.

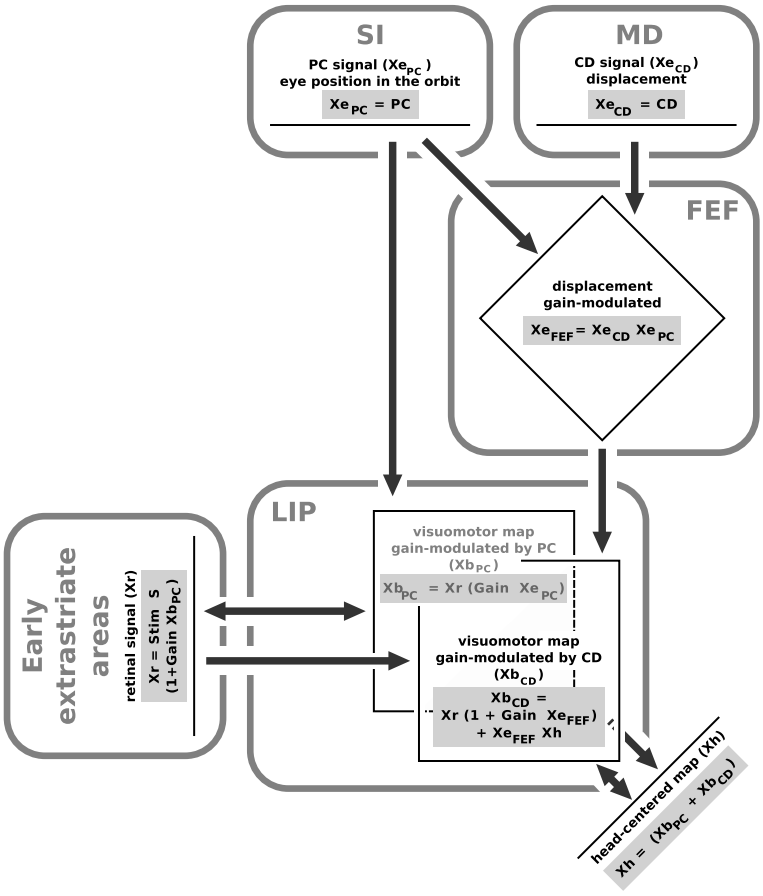

Figure 2: Our model of peri-saccadic stimulus localization is composed of three cell types, $\mathrm{Xb_{PC}}$ and $\mathrm{Xb_{CD}}$ (in LIP), which receive retinal input from early extrastriate areas as well as eye position information presumably from S1 and FEF, and Xh which encodes stimulus positions in a head-centered reference frame. The input layer (Xr) represents stimulus position retinotopically in a single dimension, modeled by Gaussian receptive fields. The stimulus signal is gain-modulated in $\mathrm{Xb_{PC}}$ by the proprioceptive eye position signal ($\mathrm{Xe_{PC}}$) and in $\mathrm{Xb_{CD}}$ by the corollary discharge ($\mathrm{Xe_{CD}}$). Both maps, $\mathrm{Xb_{PC}}$ and $\mathrm{Xb_{CD}}$ feed into the head-centered layer Xh. In order to allow interactions of these two forward connections, the maps $\mathrm{Xb_{PC}}$ and $\mathrm{Xb_{CD}}$ both encode space in the same coordinate system. Thus, the corollary discharge implicitly encodes eye position information, as motivated by an observation of Cassanello and Ferrera (2007). For simplicity, we use the same eye position signal ($\mathrm{Xe_{PC}}$) to modulate corollary discharge from MD (and SC) with eye position. The grey boxes in each layer show a simplified version of the neurons equations. In layer Xr, *Stim* is the input from earlier areas and in Xr as well as in Xh, S is the synaptic depression. In all layers, *Gain* is the gain modulation factor. PC is the proprioceptive eye position signal and CD is the corollary discharge signal.

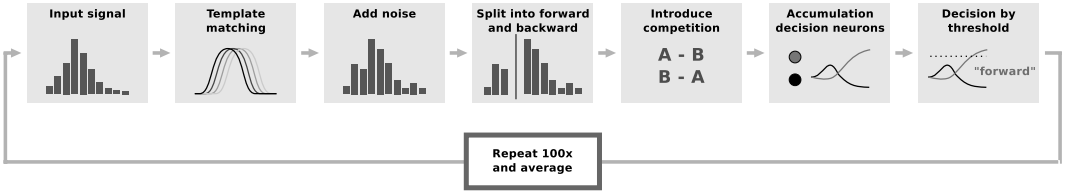

Figure 3: The decision process used in the model. It decodes the stimulus position from the activity in the head-centered map Xh. First we apply a template matching for each time step. This has the advantage of increasing the spatial resolution by using appropriate pre-calculated templates. After noise is added the noisy template matches are split into those encoding spatial positions representing a forward stimulus jump and a backward stimulus jump. The evidences for forward and backward jumps are summed up for both directions and subtracted from each other, thereby implementing a competition between both. These two values serve as input to accumulating decision neurons which compete until a threshold is reached. We repeat the entire process 100 times to yield an average percept mimicking 100 experimental trials.

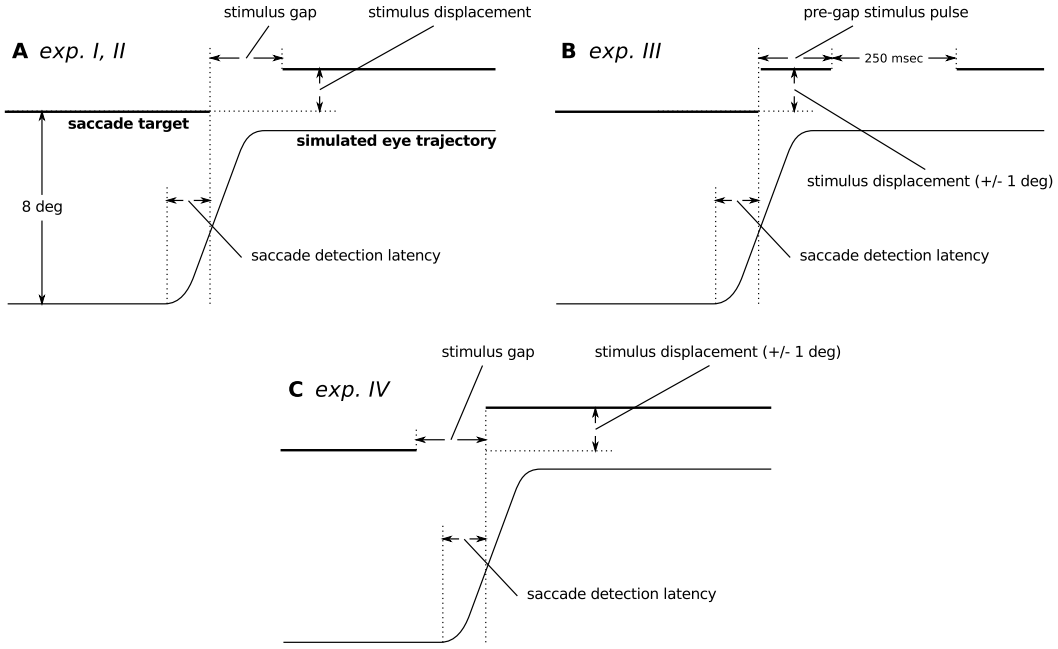

Figure 4: The experimental paradigms for saccadic suppression of displacement which we simulate. Paradigms are adopted from Deubel et al. (1996), but simplified for simulation in the model. For easy reference, we kept the original numbering of the experiments. In all experiments, we simulate saccadic eye movements from fixation at 0° towards a saccade target stimulus which is presented at a position of 8°. Spatial positions are shown on the vertical axes, time is shown on the horizontal axes. Thick lines are stimuli, thin lines are eye trajectories. In all experiments we change the scene 30ms after saccade onset. ***A***, In experiments I and II the stimulus is hidden 30ms after saccade onset. After a gap of variable length it reappears at a slightly different position. In experiment I the stimulus gap is varied (0ms, 50ms, 100ms, 180ms, or 270ms) and stimulus jumps are either $+1°$ or $-1°$. In experiment II the stimulus gap is either 0ms or 250ms and stimulus jump is varied ($-2°$, $-1°$, $0°$, $+1°$, or $+2°$). ***B***, In experiment III the stimulus jumps immediately by either $+1°$ or $-1°$ when the saccade is detected, but it is blanked again after a variable time (0ms, 25ms, 50ms, 75ms, 100ms, 125ms, or 150ms) for 250ms. We also refer to the jumped stimulus before the gap as a pre-gap stimulus pulse. ***C***, Experiment IV is similar to experiment I with the difference that the stimulus jumps when the saccade is detected (by either $+1°$ or $-1°$) but there is a stimulus gap of variable length (200ms, 180ms, 160ms, 140ms, 120ms, 100ms, 80ms, 60ms, 40ms, or 20ms) right before the stimulus jump. Thus, for most gap durations the stimulus disappears before saccade onset ("pre-gap" condition).

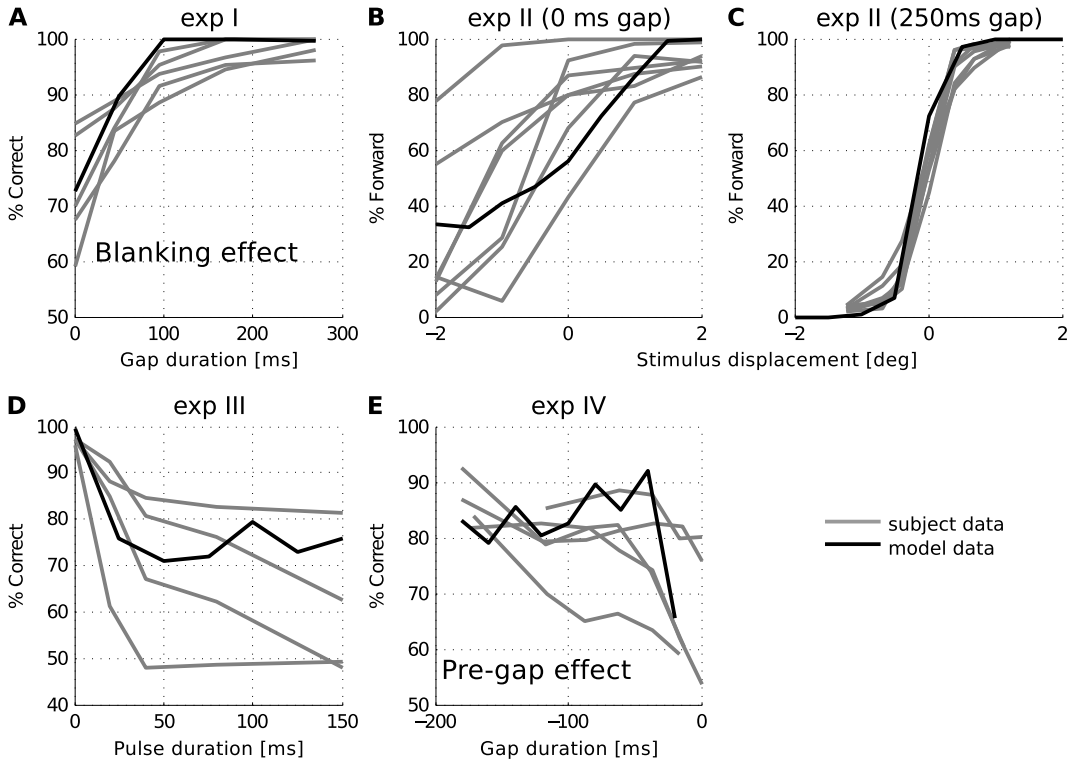

Figure 5: Comparison of subject performance and model performance. Gray lines are subjects (replotted from Deubel et al., 1996), solid lines are model performances for a decision threshold of 0.7. ***A***, Experiment I, the main finding of the blanking effect. ***B***, Experiment II with no gap. ***C***, Experiment II with a 250ms gap. ***D***, Experiment III. ***E***, Experiment IV, the main finding of the pre-gap effect.

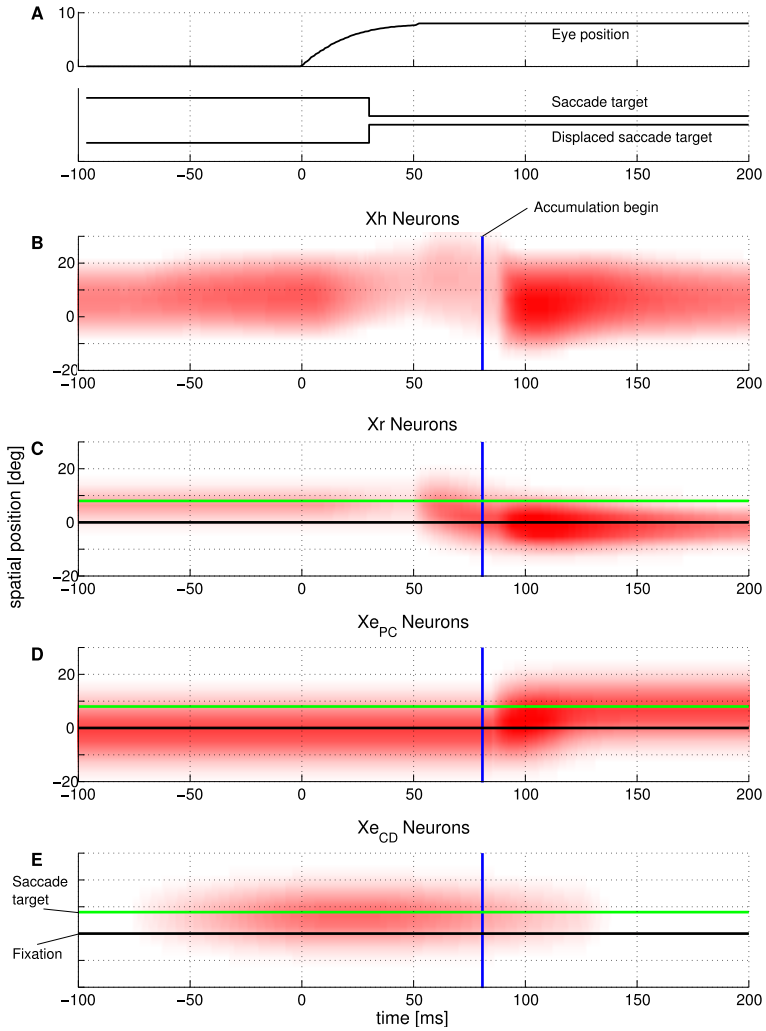

Figure 6: Activity traces of model layers for SSD simulations with 0ms gap and 0° displacement. Time relative to saccade onset is plotted on the horizontal axes, spatial position on the vertical axes. The horizontal black and green lines indicate the spatial positions of pre-saccadic fixation and planned saccade target, respectively. The vertical blue lines indicate the time where the decision process starts to accumulate evidence from Xh neurons. ***A***, Time course of events. The top graph shows the simulated eye trajectory, the middle graph shows the stimulus which is switched off 30ms after saccade onset and turned on at its displaced position the same time. ***B***, Activities of Xh neurons. They represent stimulus position in head-centered coordinates and are read out by the decision process. ***C***, Activities of Xr neurons. They represent stimulus position in retinotopic coordinates and serve as visual input to the model. ***D***, Activities of $\mathrm{Xe_{PC}}$ neurons. They represent proprioceptive eye position in the orbit (i.e. in head-centered coordinates). ***E***, Activities of $\mathrm{Xe_{CD}}$ neurons. They represent the planned saccade displacement (i.e. the planned saccade target in retinotopic coordinates).

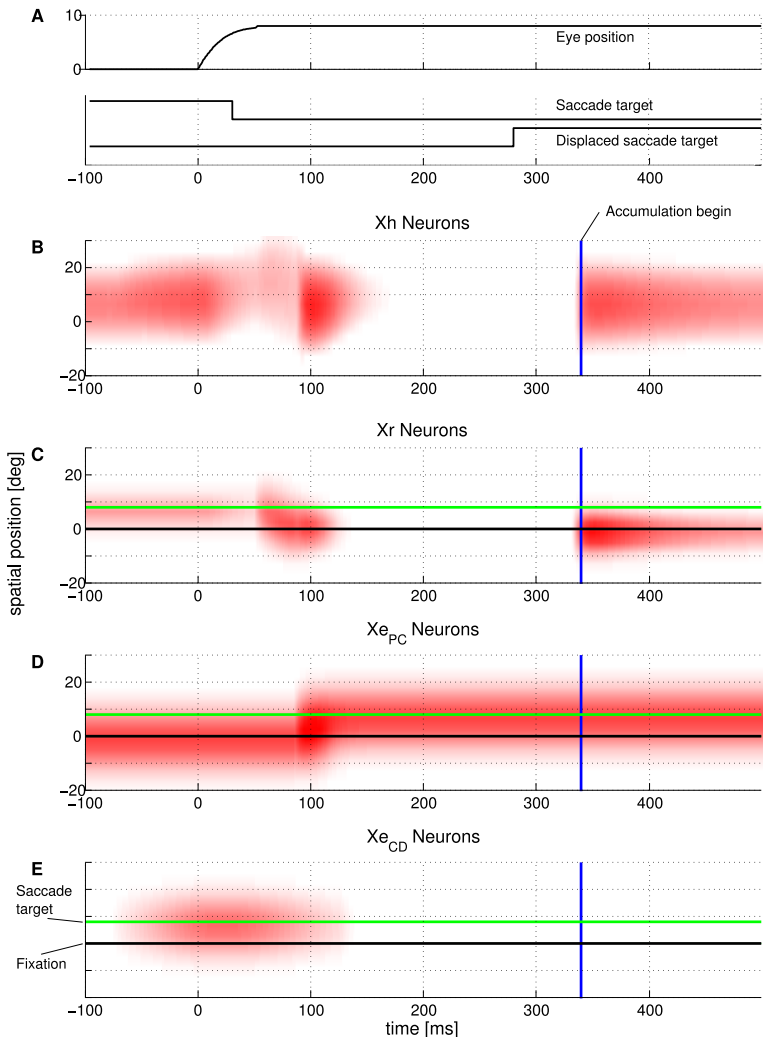

Figure 7: Activity traces of model layers for SSD simulations with 250ms gap and 0° displacement. The format is the same as in Figure 6. ***A***, The time courses of the saccade and stimulus presentation. ***B, C***, The activity traces of the head-centered output neurons in Xh and the retinal input neurons in Xr decay during the stimulus gap. When the stimulus reappears, around the time of accumulation onset (vertical blue line), all peri-saccadic perturbations in the activities are gone. ***D, E***, Activities of $\mathrm{Xe_{PC}}$ and $\mathrm{Xe_{CD}}$ neurons are identical to those in the 0ms gap condition (Figure 6).

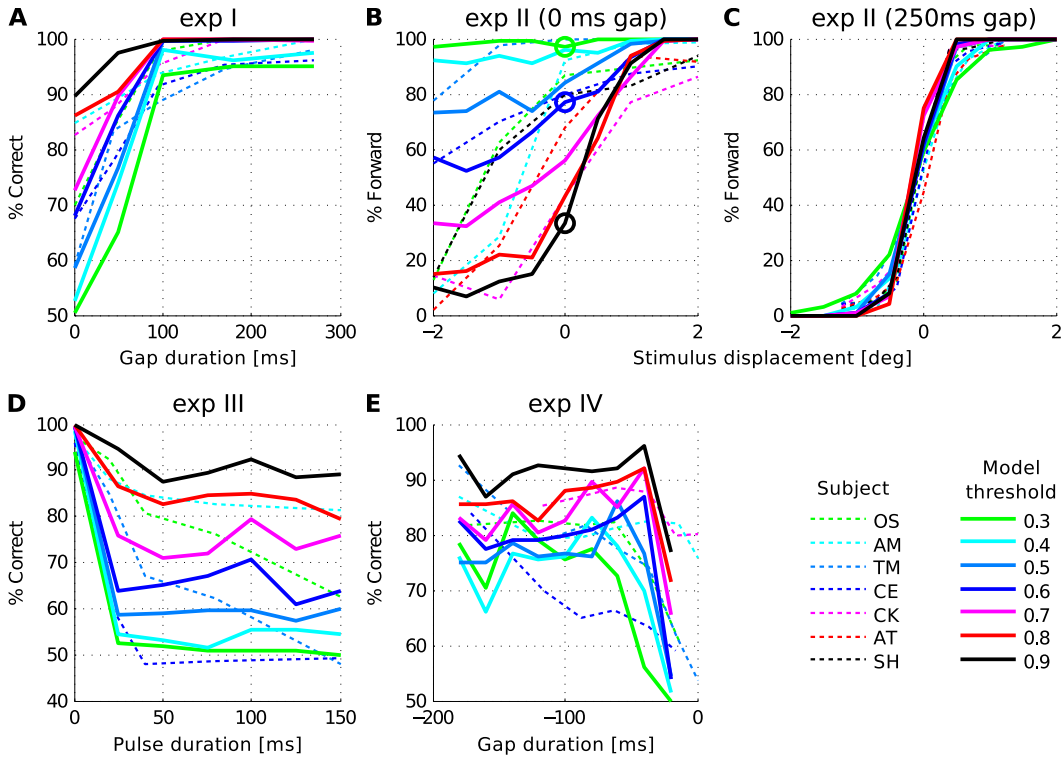

Figure 8: Comparison of subject performance and model performance. Dotted lines are subjects (replotted from Deubel et al., 1996), solid lines are model performances for different thresholds in the decision process. ***A***, Experiment I. ***B***, Experiment II with no gap. The data points marked by circles indicate the decisions which are detailed in figure 9. ***C***, Experiment II with a 250ms gap. ***D***, Experiment III. ***E***, Experiment IV.

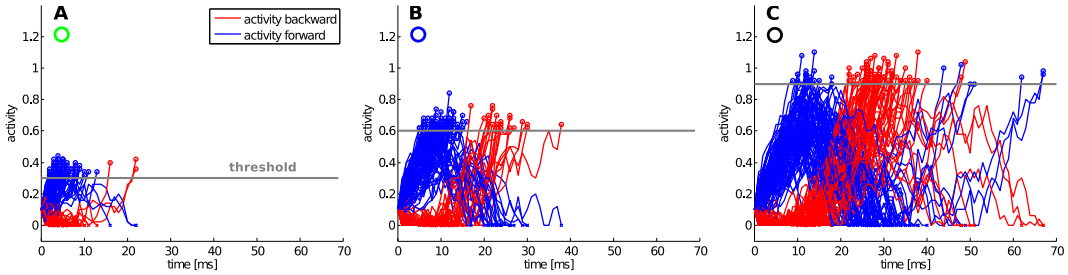

Figure 9: Activity traces of the decision neurons for SSD simulations with 0ms gap and 0° jump and different decision thresholds (0.3, 0.6, and 0.9 in panels ***A***, ***B***, and ***C*** respectively). The colored circles at the top indicate to which data point in figure 8*B* the decisions lead. Each panel shows activity traces of all 100 trials. Blue lines are the activities of the neuron representing a forward jump decision, red lines are neurons representing a 'backward jump' decision. The horizontal grey line is the decision threshold. Once either neuron's activity exceeds the threshold, it wins the trial, indicated by a circle in the color of the winning neuron. After that, the trial ends.

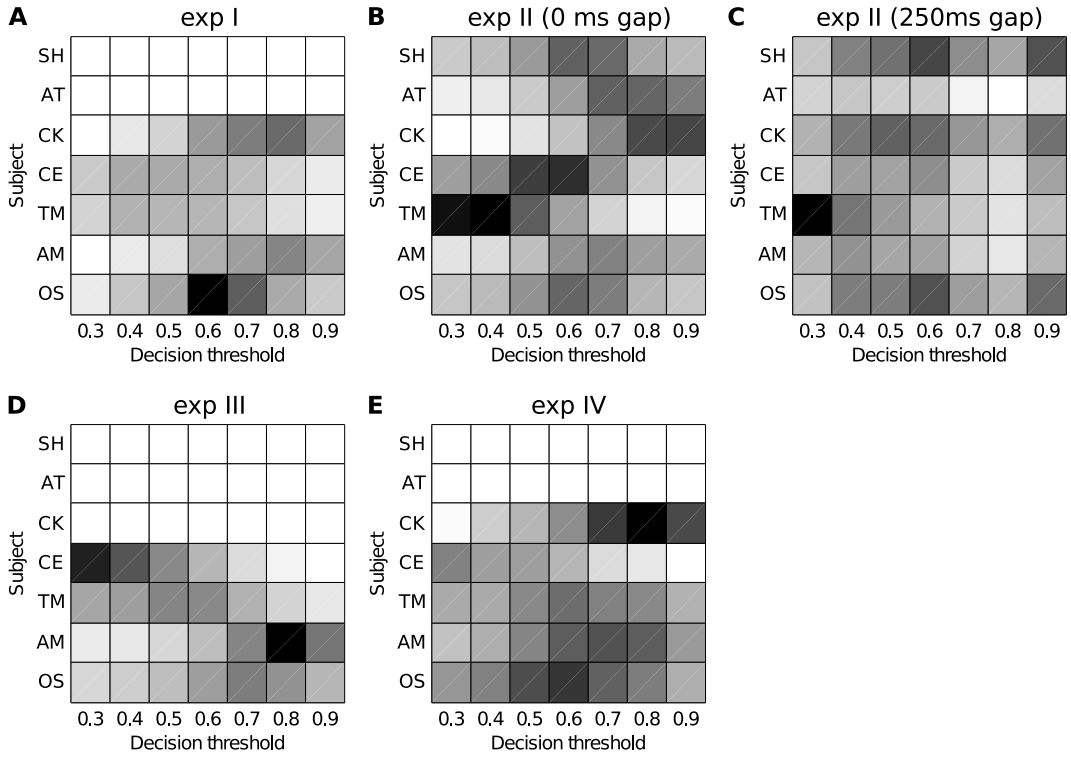

Figure 10: Comparison of subjects with model thresholds for each panel of Fig. 8. Each panel shows a matrix in which each entry indicates the mean squared error (MSE) between the subject's psychometric and the particular model's psychometric curve. Black indicates a low MSE. The typical range of best-fitting thresholds for each subject is the same across all experiments. Panels correspond to the same experiments as in Fig. 8. White rows indicate experiments in which the subject did not participate.